

Fluorescence spectral imaging for characterization of tissue based on multivariate statistical analysis

Jianan Y. Qu and Hanpeng Chang

Department of Electrical and Electronic Engineering, Hong Kong University of Science and Technology, Clear Water Bay, Kowloon, Hong Kong, China

Shengming Xiong

Institute of Optics and Electronics, Chinese Academy of Sciences, Sichuan 610209, China

Received February 1, 2002; revised manuscript received March 29, 2002; accepted April 9, 2002

A novel spectral imaging method for the classification of light-induced autofluorescence spectra based on principal component analysis (PCA), a multivariate statistical analysis technique commonly used for studying the statistical characteristics of spectral data, is proposed and investigated. A set of optical spectral filters related to the diagnostically relevant principal components is proposed to process autofluorescence signals optically and generate principal component score images of the examined tissue simultaneously. A diagnostic image is then formed on the basis of an algorithm that relates the principal component scores to tissue pathology. With autofluorescence spectral data collected from nasopharyngeal tissue *in vivo*, a set of principal component filters was designed to process the autofluorescence signal, and the PCA-based diagnostic algorithms were developed to classify the spectral signal. Simulation results demonstrate that the proposed spectral imaging system can differentiate carcinoma lesions from normal tissue with a sensitivity of 95% and specificity of 93%. The optimal design of principal filters and the optimal selection of PCA-based algorithms were investigated to improve the diagnostic accuracy. The robustness of the spectral imaging method against noise in the autofluorescence signal was studied as well. © 2002 Optical Society of America

OCIS codes: 170.0170, 110.7050, 170.3880, 170.4580, 170.6510.

1. INTRODUCTION

Light-induced fluorescence (LIF) spectroscopy is an effective and mature technique for analyzing the chemical composition of a substance of interest. Over the past two decades, it has been successfully applied in medical diagnosis with particular advantages for *in vivo* noninvasive characterization of pathological states in human tissue because of the difference between biochemical and morphological states in normal and diseased tissue reflected in the characteristics of the LIF spectral signals. Investigations of LIF spectroscopy for the diagnosis of diseased tissue have been conducted with a variety of organ sites.¹⁻³ The classification of LIF spectral signals relies on an algorithm based on the correlation between the statistical characteristics of tissue LIF spectra, such as spectral line shape and intensity, and tissue pathology.

A LIF spectrum of tissue is a multivariate function of wavelengths. To build an algorithm for classifying LIF spectral signals with minimal loss of diagnostic information, one should use multivariate statistical analysis to investigate the statistical characteristics of LIF spectral data collected from the tissue of interest. A variety of multivariate statistical analysis methods have been used in tissue spectroscopy. A comparison between different methods of classifying autofluorescence spectra is presented in Ref. 4. An algorithm based on principal component analysis (PCA) was found to produce the highest diagnostic accuracy. The commonly used multivariate

linear regression method failed to perform better than PCA when the spectral data set is not large because multivariate linear regression requires the sample number in the data set to be greater than the spectral dimensions with no collinearities in the data set.^{4,5}

PCA has been successfully applied to classifying *in vivo* autofluorescence by other groups. The results have demonstrated that PCA-based algorithms can produce high accuracy in the detection of diseased tissue because they take advantage of the diagnostic information carried in the entire LIF spectrum instead of in just a limited number of wavelength bands.⁴⁻⁸ PCA thus requires data over the entire LIF spectrum for the classification. In a standard practice of fluorescence spectroscopy with the PCA technique, the fluorescence signal must first be dispersed by a spectrograph and recorded by an array detector. An ordinary spectrometer can record only the spectrum of the fluorescence signal collected from a single pixel of the tissue image at a time. A more sophisticated imaging spectrograph with a two-dimensional detector can measure the spectra from a line over the tissue surface in one shot. The recorded spectral signals are then processed with a PCA-based algorithm to generate the diagnostic results. This pixel-by-pixel or line-by-line measurement is time consuming and may not be practical in the examination of large areas of tissue during clinical practice. However, a conventional imaging device does not record the LIF spectral signal received by each pixel of its two-dimensional

image sensor in one measurement. It is technically difficult to achieve a real-time multivariate spectral imaging.

A multivariate optical computing approach for a predictive spectroscopy has been investigated theoretically and experimentally.^{9,10} Two optical interference coatings with transmission spectra related to a regression loading are used to process an incident spectral signal and produce its score on the regression loading. To calculate the scores on i regression loadings from an incidence, $2i$ measurements are required. For a predictive spectroscopy based on the multivariate optical computing approach, all spectra from the measured samples must be excited under the same condition. However, for an imaging system the signal received by each pixel of an image sensor may vary in a wide range because the signal intensity is strongly affected by the illumination and collection geometry over the surface of the imaged object. Our group recently reported a spectral imaging method based on a different multivariate optical computing technique.¹¹ The method processes the autofluorescence with a set of optical filters correlated to the diagnostically relevant principal components (PCs) and extracts the clinically useful information with a PCA algorithm.¹¹ The major advantage of this technique is that it can process the spectral signal from the entire imaged tissue surface optically and generate the PC score images in parallel. This method makes possible the clinically desirable real-time LIF imaging of diseased tissue based on PCA.

This paper presents the results of the most recent studies. Using the *in vivo* autofluorescence of nasopharyngeal tissue, we have calculated and identified the diagnostically relevant PCs. The optical PC filters have been designed by use of commercial software for optical thin-film design. On the basis of the correlation of PC scores from the *in vivo* autofluorescence spectral data with the tissue pathology, a probability-based diagnostic algorithm and a simple threshold-based algorithm have been developed. The optical processing of autofluorescence with the designed PC filters and classification of autofluorescence with the PCA algorithms have been simulated. Factors that could affect the performance of the imaging system, such as the incident angle to the PC filters and the noise level in the autofluorescence signal, have been investigated. Finally, the performances of conventional ratio imaging systems, including the fluorescence signals in two-wavelength bands (2- λ) and three-wavelength bands (3- λ) have been evaluated for the detection of carcinoma lesions. A comparison of the ratio imaging system with 2- λ and 3- λ algorithms with the proposed PCA imaging system has been made.

2. MATERIALS AND METHODS

A. Optical Processing of Autofluorescence

PCA is a mathematical procedure that transforms a number of correlated or uncorrelated variables into a smaller number of uncorrelated variables called principal components, in which the first PC accounts for as much of the variability in the data set as possible, and each succeeding component accounts for as much of the remaining variability as possible.¹² When PCA is used to process

spectral data, it transforms the original spectral variables (wavelengths) into a set of PC spectra in the space of the original spectral variables. The PCs are arranged in the order of their contribution to the variance of the entire spectral data set. The total number of PCs generated is the same as the dimension of the original spectral data. Each original spectrum is a combination of PC loading spectra that are orthogonal to each other.

In general, the spectral characteristics of tissue are determined by a limited number of biological fluorophores and absorbers.¹ Therefore a few PCs can explain most of the informative variations in an autofluorescence spectrum, and PCA processing can dimensionally reduce the variables of the original spectral data into a small number of informative PCs that fully describe the variations in the spectral data within the limitations of noise. Scores on the diagnostically relevant PCs from the autofluorescence signals may then be related to tissue pathology and used to create a diagnostic algorithm for classifying autofluorescence signals.

To process autofluorescence and generate PC scores optically, one can design an optical filter with transmission spectra related to a PC loading spectra as

$$F_i(\lambda) = [\alpha_i PC_i(\lambda) + \beta_i] S^{-1}(\lambda),$$

subject to $0 \leq F_i(\lambda) \leq 1$, (1)

where $PC_i(\lambda)$ is the spectrum of the i th PC loading vector in the wavelength space. $S(\lambda)$ is the wavelength response of the spectral imaging system. It can be measured with a standard traceable light source. The α_i and β_i are two parameters applied to ensure that the value of $F_i(\lambda)$ falls within the range 0 to 1 because the value of $PC_i(\lambda)$ at different wavelengths could be positive or negative, but the transmission cannot be negative or greater than 1. The i th PC score from an incident spectral signal, $I(\lambda)$, can be calculated as

$$\begin{aligned} Q_i &= \int PC_i(\lambda) I(\lambda) d\lambda \\ &= \frac{1}{\alpha_i} \int I(\lambda) F_i(\lambda) S(\lambda) d\lambda \\ &\quad - \frac{\beta_i}{\alpha_i k} \int I(\lambda) F_s(\lambda) S(\lambda) d\lambda. \end{aligned} \quad (2)$$

In the first term, $\int I(\lambda) F_i(\lambda) S(\lambda) d\lambda$ is the response to spectral signal $I(\lambda)$ with PC filter $F_i(\lambda)$. In the second term, $\int I(\lambda) F_s(\lambda) S(\lambda) d\lambda$ is the response of $I(\lambda)$ with a system-response correction filter $F_s(\lambda)$ defined as $F_s(\lambda) = kS^{-1}(\lambda)$, subject to $0 \leq F_s(\lambda) \leq 1$. Here both terms in Eq. (2) are measurable. This means that, for an imaging system with $i + 1$ channels of i PC filters and one system-response correction filter, the spectral signal of each pixel can be processed in parallel optically, and the score images of all the PCs can be produced on the basis of Eq. (2) simultaneously. A diagnostic image can then be formed by use of an algorithm built on the correlation between PC scores and tissue pathology. In principle, this optical processing can completely eliminate a spectral dispersion device for recording spectral data and generating PC scores pixel-by-pixel over the entire image.

B. Principle-Component-Analysis-Based Algorithms

A diagnostic algorithm seeks to exploit the principal differences in PC scores between the autofluorescence from normal and carcinoma tissue. Since most PCs account mainly for noise and do not provide diagnostic information, it is necessary to identify a small group of informative PCs to build the algorithms to be used for classifying autofluorescence spectra. To generate the diagnostic image in real time, a good algorithm for the proposed PCA imaging system should include the minimum number of PCs without losing useful diagnostic information.

The procedure for the selection of informative PCs consists of two steps. First, the contribution of each PC to the total variance in the spectral data is proportional to its eigenvalue. High-order PCs often account for less than 1% of total data variation and represent noise. In this paper PCs that explain more than 1% of variance in the spectral data were considered to be informative PCs. In the second step, an unpaired Student's *t* test was used to evaluate the difference in projection scores on the informative PCs between the autofluorescence spectra of normal tissue and carcinoma lesions. Only the PCs that had significantly different projection scores for normal tissue and carcinoma lesions were selected for the construction of diagnostic algorithms.

After the diagnostically relevant PCs had been identified, an algorithm based on the posterior probability of the given observation being normal or carcinoma tissue was built for classification of the autofluorescence spectra. This probability-based method has been successfully applied in the autofluorescence diagnosis of cervical precancer, laryngeal lesions, and oral carcinogenesis by other groups.⁵⁻⁷ Briefly, the posterior probability of a given PC score, x_i , indicating carcinoma, C , can be estimated with Bayes theorem as follows:

$$P(C|x_i) = \frac{P(x_i|C) \times P(C) \times m}{P(x_i|C) \times P(C) \times m + P(x_i|N) \times P(N) \times \bar{m}}, \quad (3)$$

where $P(x_i|C)$ and $P(x_i|N)$ are the conditional probabilities that the PC score of a spectral data set, x_i , was collected from carcinoma tissue or normal tissue, respectively. $P(C)$ and $P(N)$ are the prior probabilities of the tissue being carcinoma or normal tissue, respectively; m is the cost of misclassification of a carcinoma as normal tissue. The sum of m and \bar{m} is equal to 1. The probability densities of PC scores are assumed to be normally distributed. The joint multivariate normal distribution for the PCs included in Eq. (3) is then

$$f(x) = \frac{I}{[(2\pi)^p |\Sigma|]^{1/2}} \exp\left[-\frac{1}{2}(x-u)'\Sigma^{-1}(x-u)\right], \quad (4)$$

where u and Σ are the mean and the covariance matrices, respectively, of the multivariate p -dimensional variable x . The dimension p is determined by the number of PCs used in the algorithm.

In a simple approach to building a PCA-based diagnostic algorithm, scores of spectral data on the diagnostically relevant PCs were used directly for classification of the autofluorescence spectra. An exhaustive search was

then conducted to find the optimal diagnostic threshold to separate the PC score of normal tissue from that of carcinoma lesions. When only one PC is included in the algorithm, the diagnostic threshold is a single point in the space of PC scores. With two or three PCs included in the algorithms, the thresholds are a line and a plane, respectively.

C. Simulation

The performance of the proposed PCA imaging system for detecting cancerous tissue was investigated by using autofluorescence spectral data collected at the nasopharyngeal tissue site *in vivo*. The details of the instrumentation for measuring LIF signals *in vivo* was reported in Ref. 13. Briefly, a mercury arc lamp filtered with a 390–450-nm bandpass filter was used as the excitation source. The excitation light was delivered to the tissue through the illumination channel of a standard nasoendoscope. The spectral response of the LIF measurement system was calibrated with a National Institute of Standards and Technology (NIST) traceable tungsten light source. The recorded LIF spectral signals from the tissues were deconvolved with the measurement system response. The autofluorescence was excited primarily by the strong spectral peaks of mercury at 404.66 and 435.84 nm. The fluorescence signals collected by the endoscope were conducted to a multichannel spectrometer with seven optical fibers that were evenly distributed in the image plane of the endoscope. This allowed investigation of the fluorescence signal received by each pixel of a two-dimensional sensor proposed for recording the LIF image from fluorescence endoscopy. The PC filters and diagnostic algorithms developed from the *in vivo* spectral data should thus be valid for a PCA imaging system with the same type of endoscope as that used for collecting the *in vivo* spectral data.

A total of 216 autofluorescence spectra were collected from 59 subjects *in vivo*. Of those, 85 measurement sites exhibited carcinoma and 131 were found to be normal tissue. Biopsy specimens were taken from the tissue sites where the autofluorescence spectra were collected, and these were subjected to histologic examinations. The raw autofluorescence signals were recorded from 470 to 680 nm with the resolution of 1.0 nm. To prepare the data for designing PC filters, the raw spectra were smoothed to remove random noise, because high-frequency spikes in the PC loadings caused by noise introduce complexity into the filter design and technical difficulties into the manufacturing the PC filters. Each smoothed spectrum was then normalized by its area to eliminate variations in measurements from site to site and from individual to individual. The smoothed and normalized spectra were used to form a preprocessed data set. The PC loadings were calculated from the preprocessed data set, and the PC filters could be designed with Eq. (1).

A cross-validation test was used to simulate the performance of the PCA spectral imaging system for classifying autofluorescence of nasopharyngeal tissue *in vivo*. In each round of the validation, one raw spectrum was kept out. The remaining 215 raw spectra were used as a training set to design PC filters and develop PCA algo-

rithms. A preprocessed data set was formed from the training set for calculating PC loadings and designing PC filters on the basis of Eq. (1). The designed PC filters were then used to process the raw spectra in the training set and produce the PC scores. Because the PCs were calculated from the preprocessed spectral data that were normalized, on the basis of Eq. (2), the i th PC score of a raw spectrum, $I(\lambda)$, can be calculated from two measurements as follows:

$$Q_i = \frac{1}{\alpha_i} \left[\frac{k \int I(\lambda) F_i(\lambda) S(\lambda) d\lambda}{\int I(\lambda) F_s(\lambda) S(\lambda) d\lambda} - \beta_i \right]. \quad (5)$$

Here the system response of $I(\lambda)$ with a correction filter $F_s(\lambda)$, $(1/k) \int I(\lambda) F_s(\lambda) S(\lambda) d\lambda$, is used for normalizing the raw spectrum, $I(\lambda)$.

In general, the spectral response of a LIF imaging system is determined mainly by the response of the image sensor in the system, usually an intensified CCD (ICCD). The spectral response of a proposed PCA imaging system, $S(\lambda)$, can be precisely measured by use of a NIST traceable tungsten light source. In the wavelength range from 470 to 680 nm, the ICCD response is a slowly varying function of the wavelength. To simplify the simulation, we assumed that $S(\lambda) = 1$ because adding a slowly varying ICCD response to the PC filters, $F_i(\lambda)$, will not

create technical complexity in the design and manufacture of filters. With the assumption of $S(\lambda) = 1$, Eq. (5) becomes

$$Q_i = \frac{1}{\alpha_i} \left[\frac{\int F_i(\lambda) I(\lambda) d\lambda}{\int I(\lambda) d\lambda} - \beta_i \right]. \quad (6)$$

To build a PCA algorithm, the PC scores calculated from the training set based on Eq. (6) were correlated with tissue pathology as discussed in Subsection 2.B. The kept-out raw spectrum was then processed by the designed PC filters and classified by the PCA algorithm. This process was repeated until all the 216 raw spectra had been classified. In each round of the cross validation, a new set of PC filters and a new algorithm were created by use of the training data set. The sensitivity and specificity of the PCA imaging system for detection of carcinoma lesions were calculated on the basis of the classification of a kept-out raw spectrum in each round of cross validation.

3. RESULTS AND DISCUSSION

Typical *in vivo* autofluorescence spectra before and after preprocessing are displayed in Fig. 1. A MATLAB-based PCA program was developed to calculate the PCs by use

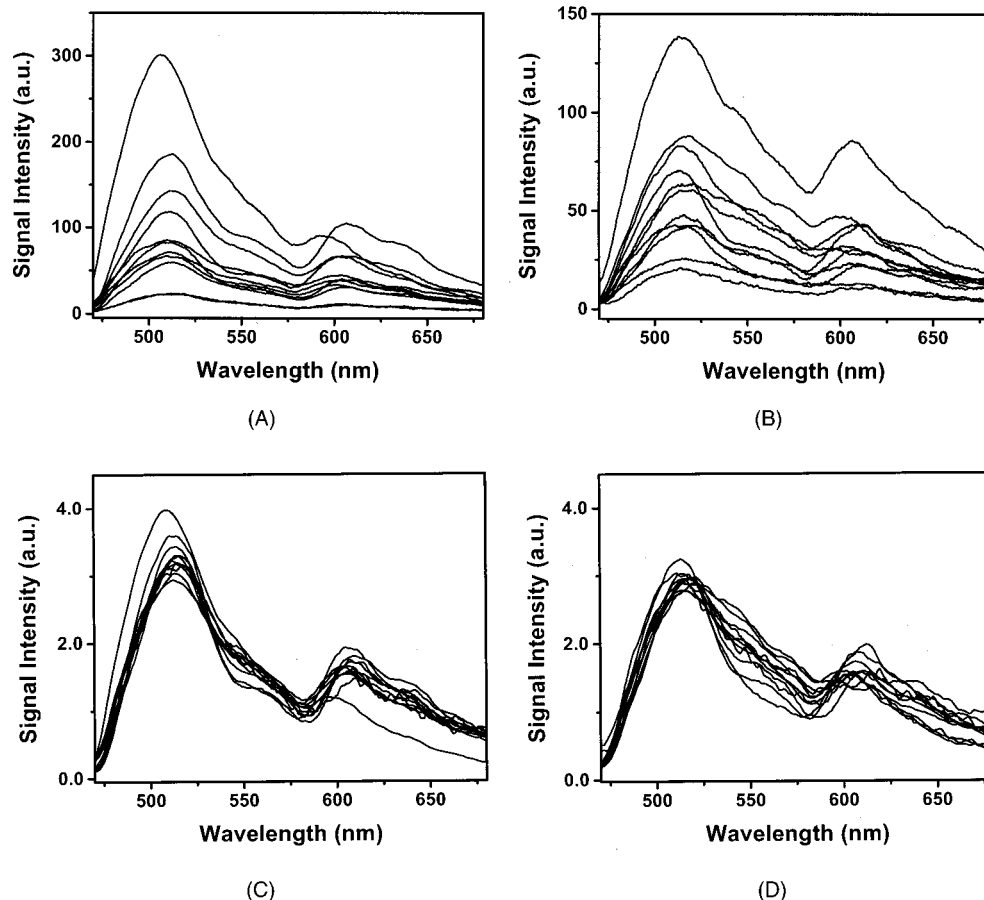


Fig. 1. Typical raw and preprocessed LIF spectra. Before preprocessing: (A) normal tissue and (B) carcinoma. After preprocessing: (C) normal tissue and (D) carcinoma.

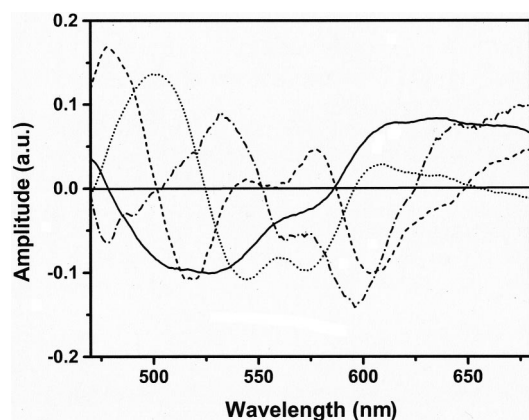


Fig. 2. Spectra of the first four principal component loadings. Solid curve, PC1; dotted curve, PC2; dashed curve, PC3; dashed-dotted curve, PC4.

of the preprocessed data set. It was found that the first four PCs accounted for over 98% of the total data variance. The result demonstrates again that the significant data variation can be described by a few informative PCs because the spectral characteristics of autofluorescence are determined by a few dominant biological fluorophores and absorbers. The higher-order PCs mainly account for random noise and do not contain diagnostic information.

The first four PC loadings obtained from all 216 spectra are shown in Fig. 2. To identify further the diagnostically relevant PCs from the informative PCs, an unpaired Student's t test was conducted on the hypothesis that there is an equal mean PC score between the autofluorescence spectra collected from normal tissue and from carcinoma lesions. The small p value for the first two PCs (p value $\ll 0.001$) shows that there is significant statistical difference in the PC1 and PC2 scores between normal tissue and carcinoma lesions. The p values for PC3 and PC4 were 0.28 and 0.49, respectively. This means that the differences in PC3 and PC4 scores between the spectra from normal tissue and carcinoma lesions are not statistically significant. Therefore PC3 and PC4 do not carry the necessary diagnostic information for separating carcinoma lesions from normal tissue. Only the first two PCs should be included in a PCA algorithm.

Some statistical characteristics of autofluorescence can be found in Fig. 2. The relatively high negative value of PC1 from 500 to 550 nm and the high positive value from 600 to 650 nm suggest that PC1 mainly captures the difference in the spectral data between these two wavelength regions. The blood-absorption spectrum in the range 525–590 nm is reflected in the PC2 spectrum, which suggests that the variations of blood content in tissues is included in PC2.

Optical PC filters based on the assumption that $S(\lambda) = 1$ were designed with commercial software for optical thin-film design (Film Wizard, Scientific Computing International, California). Commonly used materials for manufacturing interference filters were chosen in the design. The substrate material was SiO_2 glass. SiO_2 and TiO_2 were selected for the low-index coating layer and for the high-index coating layer, respectively. The values of the parameters, α_i and β_i , were chosen to keep the transmissions of the PC1 and PC2 filters in the range of 10% to

90%. By use of the optimization methods provided by the software (Simplex and Global Modified Levenberg–Marquardt), the filter structures were determined in terms of the number of coating layers and the thickness of each layer to produce transmission to fit that of a PC filter calculated by use of Eq. (1) with the assumption that $S(\lambda) = 1$. Because coating thickness can be controlled at the angstrom level for a commercial coater, the minimum thickness of each coating was set to 15 nm to ensure that the designed filters can be manufactured without technical obstacles. The optimal number of coating layers for PC1 and PC2 filters was found to be 22 and 32, respectively. The coating thickness for PC1 and PC2 filters ranged from 17.12 to 671.61 nm and 16.19 to 849.00 nm, respectively. As shown in Fig. 3, the transmissions of the designed optimal thin-film filters fit well to those of the calculated PC1 and PC2 filters. The scores on PC1 and PC2 from the raw autofluorescence spectra were then calculated by use of Eq. (6) with the transmission spectra of the designed PC1 and PC2 filters shown in Fig. 3.

To calculate the posterior probability for spectral classification, we determined the conditional probabilities for the normal tissue group and the carcinoma group in Eq. (3) by fitting a normal probability density function to each PC score. The joint distribution for PC1 and PC2 scores was then determined with Eq. (4). By use of the data set with all 216 spectra, the calculated posterior probabilities that a given sample belongs to the carcinoma group by use of PC1 and PC2 are shown in Fig. 4. In this self-validation, it was found that the total number of misclassified samples was minimized when the cost of misclassification was set to 0.6. As can be seen, most normal tissue and carcinoma lesions were well separated on the basis of the posterior probability that reveals the certainty of a specific sample belonging to the group of normal tissues or carcinoma lesions. However, there were a

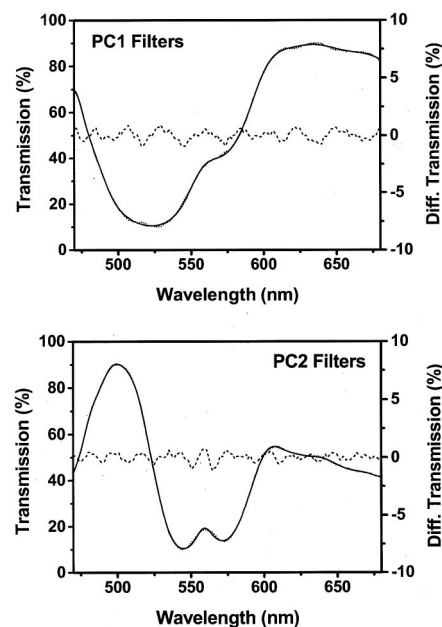


Fig. 3. Transmission curves of designed and calculated PC filters. Solid curves, designed filters; dotted curves, calculated filters; dashed curves, differential transmissions between designed filters and calculated filters.

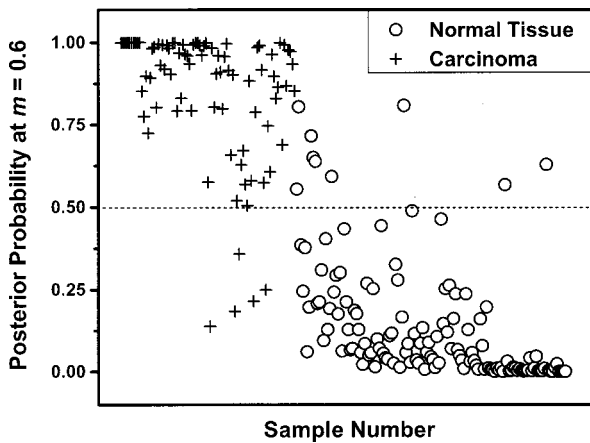


Fig. 4. Posterior probability of a given tissue belonging to the carcinoma group on the basis of PC1 and PC2 scores.

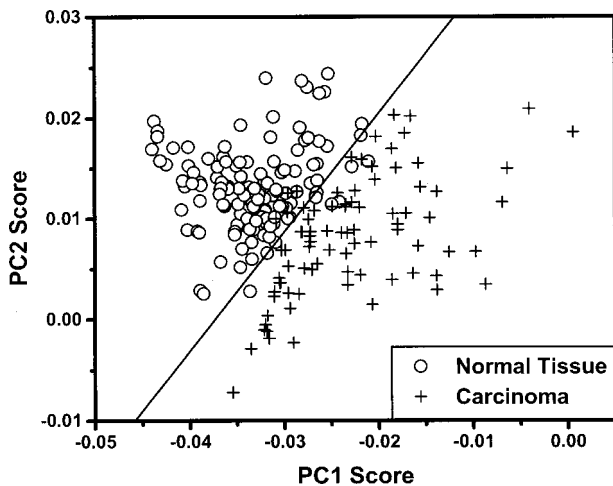


Fig. 5. Scatter plot of the PC1 score versus the PC2 score.

small number of observations that significantly deviated from the majority. This makes it impossible to set a diagnostic threshold able to separate completely normal tissues from carcinoma lesions. In practice, a diagnostic algorithm of any desired sensitivity or specification for classifying *in vivo* autofluorescence spectra can be obtained by varying the misclassification cost, m . When the total misclassified samples were minimized with setting m to 0.6 in the self-validation, the sensitivity and specificity were found to be 94% and 93%, respectively.

In a threshold-based approach, the diagnostic algorithm was built with the first two PCs. The scatter plot of the PC1 and PC2 scores calculated from Eq. (6) with the designed PC filters is shown in Fig. 5. In the two-dimensional space of PC1 and PC2 scores, a diagnostic threshold line defined as $Y = aX + b$ was developed to separate the scores of carcinoma spectra from those of normal tissue and to create a diagnostic algorithm, where X and Y are the PC1 and PC2 scores. Accuracy in separating carcinoma from normal tissue is controlled by choosing the parameters a and b . A sensitivity was set, and then an exhaustive search was performed to determine the values of a and b that maximized the specificity corresponding to the chosen sensitivity. As an example,

a diagnostic line classifying the carcinoma spectra at a sensitivity of 94% and the specificity of 96.5% is depicted in Fig. 5. Here the data set with all the 216 spectra was used for the self-validation.

To evaluate the performance of a PCA imaging system with the probability-based algorithm and the threshold-based algorithm, cross validations were conducted. The sensitivity for classifying the spectral data in the training set by each algorithm in each round of cross validation were set to be 97%, 95%, and 93%. The maximal specificity corresponding to each preset sensitivity for the probability-based PCA method was calculated by varying the cost of misclassification in Eq. (3). For the threshold-based algorithm, the slope and Y-axis intercept of the diagnostic line were adjusted to maximize the specificity. The results are shown in Table 1. The sensitivity and specificity for the prediction set shown in Table 1 were calculated from the classification of kept-out sample in 216 rounds of cross validation. The comparison in Table 1 shows that threshold-based algorithm produces higher diagnostic accuracy than the probability-based algorithm in all instances.

In principle, the probability-based method can include an unlimited number of diagnostically relevant PCs in the spectral analysis. It is convenient to use the resulting posterior probability ranging from 0 to 100% for the classification of the autofluorescence spectra. However, the performance of the algorithm relies on the accuracy in the estimation of the PC score density function.¹⁴ With an increasing number of PCs included in the algorithm, the dimension of the score probability density function increases. When the total number of samples is not large enough, the accuracy of density estimation by use of Eq. (4) drops. Furthermore, the probability-based algorithm may be corrupted when the score probability density function deviates significantly from the normal distribution. The major advantage of a threshold-based algorithm is that it is independent of the score probability density function. The disadvantage is that the exhaustive search may be time consuming and not accurate in finding the optimal diagnostic threshold when the sample volume is limited and the algorithm included too many PCs.

The normality of the PC1 and PC2 score distributions was tested for the normal tissue and carcinoma samples. A $Q-Q$ plot correlation coefficient method was used to assess the assumption of normality.¹⁵ The normality assumption was found to hold for the PC1 scores of normal tissue and the PC2 scores of both normal tissue and car-

Table 1. Sensitivity/Specificity (%) of the Probability-Based Algorithm and the Threshold-Based Algorithm for Self-Calibration in Training Sets and the Prediction of Kept-Out Samples

Self-Calibration in Training Sets		Prediction of Kept-Out Samples	
Probability	Threshold	Probability	Threshold
97/79	97/85	97/78	97/84
95/90	95/95	95/90	95/93
93/94	93/97	93/93	93/95

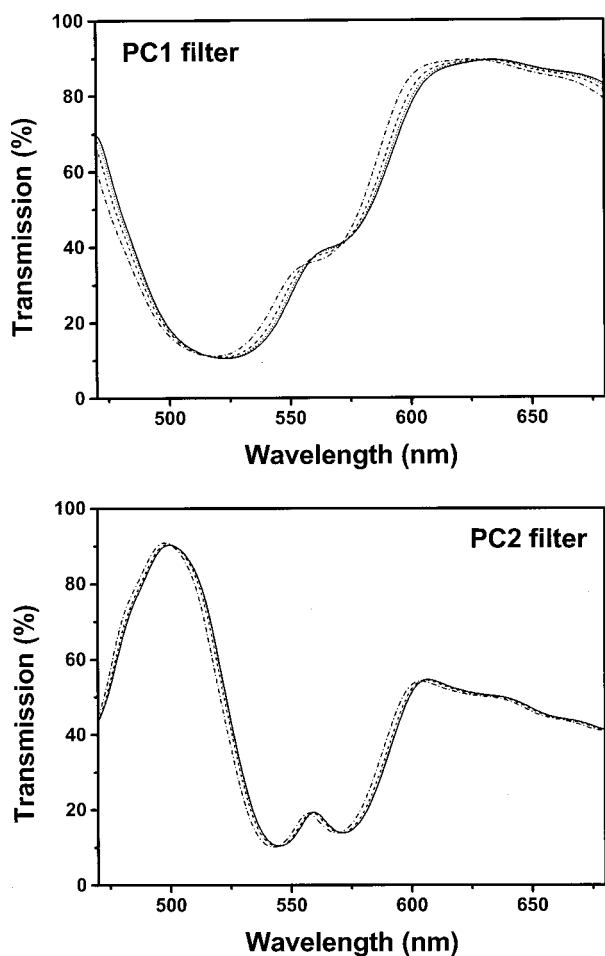


Fig. 6. Transmissions of the designed PC filters at different incident angles. Solid curves, 0 deg; dotted curves, 3 deg; dashed curves, 6 deg; dashed-dotted curves, 10 deg.

cinoma lesions. However, the normality assumption did not hold for the PC1 scores of the carcinoma lesions. This indicates that the PC1 scores for the carcinoma lesions were not normally distributed. Therefore the assumption of a normal distribution for the PC1 scores from carcinoma tissue may contribute to misclassification of the fluorescence spectral data. This may explain why the diagnostic accuracy of the threshold-based algorithm is higher than that of the probability-based algorithm.

In designing the PC filters, the incidence was assumed to be normal to the filter. However, for a realistic imaging system, the incidence will be within a range of a few degrees from the normal of the filter no matter where the filter is placed in the system. Because the transmission spectrum of an interference filter shifts with a change of incident angle, the PC score value from a LIF signal will then not be the same when the incident light comes from different angles. Figure 6 displays the transmission spectra of the designed PC filters at different incident angles. As can be seen, a shift of the transmission spectrum to short wavelengths becomes obvious when the incident angle is increased to 6 deg. The transmission shift will create error in the generation of the PC score. The extent to which the incident angle would affect the performance of the proposed PCA imaging system was investigated.

The spectra data were processed with transmissions at different angles from the PC filters designed for 0-deg incidence by use of Eq. (6). A threshold algorithm with 94% sensitivity and 96% specificity developed from a 0-deg incident angle was used to classify the spectral scores generated by the PC filters at different angles. Here a self-validation is used. In the 0-nm shift row in Table 2, the degradation of the diagnostic algorithm caused by the different incident angles is demonstrated. As can be seen, the degradation was not significant when the incident angle was smaller than 3 deg. However, the algorithm begins to corrupt completely when the incident angle is greater than 7.5 deg. This was caused by the wavelength shift of PC filters at large incident angles.

To build a realistic and compact PCA imaging system, it is desirable to have PC filters with a large acceptance angle to reduce the effect of the incident angle on system performance. A series of filters was designed with the same transmission spectral shape as the PC filters, but the spectra were shifted to the longer wavelengths to compensate for the blueshift caused by increasing incident angle. Specifically, the shift was set to 0.5 and 1 nm. The same threshold algorithm with 94% sensitivity and 96% specificity was used to classify the scores generated by the redshifted PC filters, and the results are shown in the 0.5-nm shift and the 1-nm shift rows of Table 2. It was found that the performance of the PCA imaging with 0.5-nm redshifted PC filters was improved compared with that with nonshifted filters. The acceptance angle of the PCA imaging system was increased approximately up to a factor of 2 over the acceptance angle of that with nonshifted PC filters without sacrificing much sensitivity and specificity. The results in the 1-nm shift row of Table 2 show that 1-nm redshifted PC filters overcompensated for the blueshift caused by the incident angle, because the performance at 0-deg incident angle decreased significantly, although the system performed better at large incident angles.

It should be noted that the fluorescence signal varies from individual to individual and is strongly dependent on the illumination and collection geometry. In the measurement of autofluorescence from a nasopharyngeal site *in vivo*, the LIF signals captured by the ICCD were averaged over four frames to improve the signal-to-noise ratio (SNR). This may not be possible with a real-time PCA imaging system. Also, the distance between the distal tip of the endoscope and the tissue surface was well controlled to ensure a good SNR in the collected LIF signals. However, for a realistic LIF imaging system, the SNR of image pixels may vary over a large range because the ir-

Table 2. Sensitivity/Specificity (%) of the Spectral Classification by Use of PC Filters with Different Transmission Shifts at Different Angles

Transmission Shift (nm)	Incident Angle					
	0°	3°	4.5°	6°	7.5°	10°
0	94/96	94/94	95/91	95/90	95/87	99/74
0.5	93/96	94/96	94/95	95/93	95/91	98/80
1	90/97	92/97	93/96	94/96	95/92	95/86

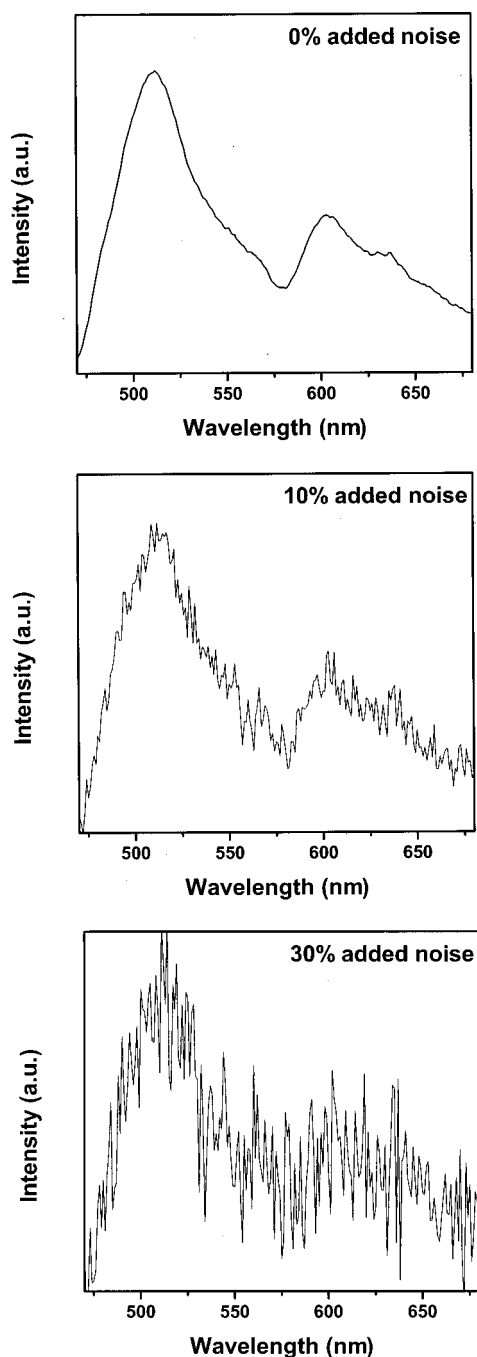


Fig. 7. Typical spectra with added Gaussian random noise.

regularity of the tissue surface causes great nonuniformity of illumination and collection geometry over the imaged tissue surface. The SNR could be high in the area close to the distal tip of the endoscope. However, the SNR could also be poor. Here the performance of the PCA imaging system in classifying noisy LIF signals was evaluated. The designed PC filters equipped with the PCA imaging system were based on autofluorescence spectra with high SNR.

To simulate the classification of a noisy LIF signal, different amounts of Gaussian random noise were added to the kept-out spectrum in each round of cross validation. The amplitude of the added noise was set to 5%, 10%,

20%, and 30% of the average amplitude of the kept-out spectrum, respectively. Typical spectra with added noise are shown in Fig. 7. The procedures to design PC filters and develop PCA algorithms with the data in the training set were the same as in the previously discussed cross validation. It should be emphasized again that the data in the training set were raw spectra with high SNR. The sensitivity and specificity were calculated through the classification of kept-out samples with added noise in 216 rounds of cross validation. The results are displayed in Table 3. Here the threshold-based algorithm was used. The sensitivity of the algorithm for the training set was set to 94%. As can be seen, even when the PC filters and PCA algorithm were built on high-SNR data, the diagnostic accuracy was not significantly affected when the noise level was lower than 20%. However, the degradation of the system performance becomes obvious when the noise level was greater than 30%.

To compare the PCA imaging method with the conventional ratio imaging methods by use of the signals at two wavelengths (2- λ) or three wavelengths (3- λ) for classification of LIF spectra, the characteristics of 216 *in vivo* fluorescence spectra were studied to identify the wavelength bands that optimally separate the carcinoma lesions from normal tissues. Detailed procedures to develop 2- λ and 3- λ algorithms have been reported in Ref. 13. Briefly, for a 2- λ algorithm, the discrimination between normal and carcinoma tissue is based on the difference in the ratio between the spectral signals at two wavelength bands. An exhaustive search was conducted to find the wavelength bands that have ratio values with the most significant statistical difference between carcinoma and normal samples. The optimal wavelength bands for the 2- λ algorithm was found to be 505 ± 20 and 605 ± 40 nm. For the 3- λ algorithm, the effect of blood absorption on the spectral characteristics is taken into account, because blood has strong absorption in the wavelength region of 530–590 nm. The optimal wavelength bands were found to be 510 ± 20 , 550 ± 20 , and 610 ± 40 nm.

The diagnostic accuracy of 2- λ and 3- λ algorithms was evaluated by use of cross validation. In a comparison with the performance of the PCA-based algorithms shown in Table 1, when the sensitivity of the 2- λ algorithm developed from the training set in each round of cross validation was set to 97%, 95%, and 93%, the sensitivity and specificities calculated from the classification of kept-out samples were 97% and 77%, 94% and 83%, and 91% and 89%, respectively. It was found that there was no improvement in classification accuracy from the 3- λ algorithm over that from the 2- λ algorithm. As can be seen, the PCA-based algorithms demonstrate an obvious ad-

Table 3. Accuracy of the Spectral Classification at Different Noise Levels

Added Noise	Percentage of Added Noise				
	0	5	10	20	30
Sensitivity	93	93	93	92	91
Specificity	95	95	95	94	92

vantage in classification accuracy over the 2- λ and 3- λ algorithms because the PCA methods utilize the information carried across the entire fluorescence spectra instead of a limited number of wavelength bands.

4. CONCLUSION

An optical processing method based on PCA is proposed for the classification of autofluorescence and the characterization of tissue. The major advantage of this method is that it completely eliminates the dispersion instrument and computer processing required to generate PC scores. This parallel processing method could be used in a multi-channel imaging system to generate multiple PC score images simultaneously and form a diagnostic image with a PC-score-based algorithm. The proposed PCA imaging technique could tremendously increase system sensitivity, because the fluorescence signal is processed and recorded directly by an image sensor instead of being dispersed and distributed to many pixels of the array sensor by a spectrograph as in traditional PCA methods.

By using autofluorescence spectral data collected from nasopharyngeal tissue *in vivo*, PC filters have been designed with commonly used optical coating materials and manufacturable coating structures. The optical processing of autofluorescence signals was simulated with these PC filters, and PCA-based algorithms were developed from the PC scores generated by the optical processing. The results demonstrated that the PCA imaging method could produce high sensitivity and specificity in differentiating carcinoma lesions from normal tissue. The threshold-based PCA algorithm performed better than the probability-based PCA algorithm because it is independent of PC score distributions.

The effects of incident angle and the SNR of the fluorescence on the performance of the PCA imaging system were investigated. It was found that, with optimal design, the acceptance angle of the PC filter could be significantly increased without sacrificing system performance. The PCA algorithm remained accurate when the noise level in the fluorescence spectral signal was not more than 20%. In a comparison with the previously reported 2- λ and 3- λ algorithms, the PCA imaging method was found to be capable of producing higher diagnostic accuracy by taking advantage of the diagnostic information carried across the entire spectrum.

ACKNOWLEDGMENT

The authors acknowledge the support received from the Hong Kong Research Grants Council through grant HKUST6052/00M.

Address correspondence to J. Y. Qu at the address on the title page or by e-mail at eequ@ust.hk.

REFERENCES

1. R. Richards-Kortum and E. Sevick-Muraca, "Quantitative optical spectroscopy for tissue diagnosis," *Annu. Rev. Phys. Chem.* **47**, 555–606 (1996).
2. S. Andersson-Engels, C. Klinteberg, K. Svanberg, and S. Svanberg, "*In vivo* fluorescence imaging for tissue diagnostics," *Phys. Med. Biol.* **42**, 815–824 (1997).
3. G. A. Wagnieres, W. M. Star, and B. C. Wilson, "*In vivo* fluorescence spectroscopy and imaging for oncological applications," *Photochem. Photobiol.* **68**, 603–632 (1998).
4. K. M. O'Brien, A. F. Gmitro, G. R. Gindi, M. L. Stetz, F. W. Cutruzzola, L. I. Laifer, and L. L. Deckelbarm, "Development and evaluation of classification algorithms for fluorescence guided laser angioplasty," *IEEE Trans. Biomed. Eng.* **36**, 424–431 (1989).
5. C. Eker, R. Rydell, K. Svanberg, and S. Andersson-Engels, "Multivariate analysis of laryngeal fluorescence spectra recorded *in vivo*," *Lasers Surg. Med.* **28**, 259–266 (2001).
6. N. Ramanujam, M. F. Mitchell, A. Mahadevan, S. Thomsen, A. Malpica, T. Wright, N. Atkinson, and R. Richards-Kortum, "Development of a multivariate statistical algorithm to analyze human cervical tissue," *Lasers Surg. Med.* **19**, 46–62 (1996).
7. C. Y. Wang, C. T. Chen, C. P. Chiang, S. T. Young, S. N. Chow, and H. K. Chiang, "A probability-based multivariate statistical algorithm for autofluorescence spectroscopic identification of oral carcinogenesis," *Photochem. Photobiol.* **69**, 471–477 (1999).
8. E. B. Hanlon, I. Itzkan, R. R. Dasari, M. S. Feld, R. J. Ferrante, A. C. McKee, D. Lathi, and N. W. Kowall, "Near-infrared fluorescence spectroscopy detects Alzheimer's disease *in vitro*," *Photochem. Photobiol.* **70**, 236–242 (1999).
9. M. P. Nelson, J. F. Aust, J. A. Dobrowolski, P. G. Verly, and M. L. Myrick, "Multivariate optical computation for predictive spectroscopy," *Anal. Chem.* **70**, 73–78 (1998).
10. O. Soyemi, D. Eastwood, L. Zhang, H. Li, J. Karunamuni, P. Gemperline, R. A. Synowicki, and M. L. Myrick, "Design and testing of a multivariate optical element: the first demonstration of multivariate optical computing for predictive spectroscopy," *Anal. Chem.* **73**, 1069–1079 (2001).
11. J. Y. Qu, H. Chang, and S. Xiong, "Optical processing of light induced autofluorescence for characterization of tissue pathology," *Opt. Lett.* **26**, 1268–1270 (2001).
12. J. E. Jackson, *A User's Guide to Principal Components* (Wiley, New York, 1991).
13. J. Y. Qu, P. W. Yuen, Z. J. Huang, D. Kwong, J. Shan, S. J. Lee, W. K. Ho, and W. I. Wei, "Preliminary study of *in vivo* autofluorescence of nasopharyngeal carcinoma and normal tissue," *Lasers Surg. Med.* **26**, 432–440 (2000).
14. B. W. Silverman, *Density Estimation for Statistics and Data Analysis* (Chapman & Hall, New York, 1986).
15. A. J. Richard and W. W. Dean, *Applied Multivariate Statistical Analysis* (Prentice-Hall, Englewood Cliffs, N.J., 1998).